

See discussions, stats, and author profiles for this publication at: <https://www.researchgate.net/publication/7343282>

# Polyelectrolyte Multilayers with a Tunable Young's Modulus: Influence of Film Stiffness on Cell Adhesion

ARTICLE in LANGMUIR · FEBRUARY 2006

Impact Factor: 4.46 · DOI: 10.1021/la0521802 · Source: PubMed

CITATIONS

191

READS

141

10 AUTHORS, INCLUDING:



**Aurore Schneider**

European Patent Office (EPO) Netherlands

13 PUBLICATIONS 890 CITATIONS

SEE PROFILE



**Grégory Francius**

French National Centre for Scientific Research

66 PUBLICATIONS 1,282 CITATIONS

SEE PROFILE



**Benoit Frisch**

French National Centre for Scientific Research

90 PUBLICATIONS 2,492 CITATIONS

SEE PROFILE



**Catherine Picart**

Ecole de Physique, Electronique et Matériaux...

146 PUBLICATIONS 7,383 CITATIONS

SEE PROFILE

## Polyelectrolyte Multilayers with a Tunable Young's Modulus: Influence of Film Stiffness on Cell Adhesion

Aurore Schneider,<sup>†</sup> Grégory Francius,<sup>†</sup> Rodolphe Obeid,<sup>†</sup> Pascale Schwinté,<sup>‡</sup>  
Joseph Hemmerlé,<sup>†</sup> Benoît Frisch,<sup>§</sup> Pierre Schaaf,<sup>||</sup> Jean-Claude Voegel,<sup>†</sup>  
Bernard Senger,<sup>†</sup> and Catherine Picart<sup>\*,†</sup>

*Institut National de la Santé et de la Recherche Médicale, Unité 595, Faculté de Chirurgie Dentaire, Université Louis Pasteur, 11 rue Humann, 67085 Strasbourg Cedex, France, Albert-Ludwigs-Universität, Institut für Molekulare Medizin und Zellforschung, Sektion Biophysik, Hermann-Herderstrasse 9, 79104 Freiburg, Germany, Laboratoire de Chimie Bioorganique, UMR 7514 CNRS-ULP, Faculté de Pharmacie, 74 route du Rhin, 67400 Illkirch, France, and Institut Charles Sadron, Centre National de la Recherche Scientifique, Université Louis Pasteur, 6 rue Boussingault, 67083 Strasbourg Cedex, France*

Received August 10, 2005. In Final Form: October 7, 2005

Mechanical properties of model and natural gels have recently been demonstrated to play an important role in various cellular processes such as adhesion, proliferation, and differentiation, besides events triggered by chemical ligands. Understanding the biomaterial/cell interface is particularly important in many tissue engineering applications and in implant surgery. One of the final goals would be to control cellular processes precisely at the biomaterial surface and to guide tissue regeneration. In this work, we investigate the substrate mechanical effect on cell adhesion for thin polyelectrolyte multilayer (PEM) films, which can be easily deposited on any type of material. The films were cross linked by means of a water-soluble carbodiimide (EDC), and the film elastic modulus was determined using the AFM nanoindentation technique with a colloidal probe. The Young's modulus could be varied over 2 orders of magnitude (from 3 to 400 kPa) for wet poly(L-lysine)/hyaluronan (PLL/HA) films by changing the EDC concentration. The chemical changes upon cross linking were characterized by means of Fourier transform infrared spectroscopy (FTIR). We demonstrated that the adhesion and spreading of human chondrosarcoma cells directly depend on the Young's modulus. These data indicate that, besides the chemical properties of the polyelectrolytes, the substrate mechanics of PEM films is an important parameter influencing cell adhesion and that PEM offer a new way to prepare thin films of tunable mechanical properties with large potential biomedical applications including drug release.

### Introduction

Recently, the role of substrate elasticity on several cell properties such as adhesion, differentiation, migration, and spreading has been shown for various cell types cultured on different substrates.<sup>1–6</sup> Besides surface chemistry and topography, which have been widely investigated and are recognized as being important factors in cellular processes, new findings regarding the importance of the pure mechanical properties of a material open new possibilities. In particular, in the field of biomaterials, controlling the surface mechanical properties may be a means of influencing cell behavior including recolonization, adhesion, and migration. Such an approach has recently been investigated for myotube cultures on polyacrylamide (PAAM) gels of tunable elasticity.<sup>7</sup> Usually, these studies deal with “model” 3D gels of polyacrylamide and poly(dimethylsiloxane) (PDMS), which can

be prepared easily and whose elasticity can be tuned by varying the cross-linker concentration.<sup>8,9</sup> However, such model substrates are not designated to be used in future in vivo applications. In recent works, gels made of the biopolymer alginate, which is commonly employed in tissue engineering applications, were also used to investigate the relation between chondrocyte and myoblast adhesion and gel elasticity.<sup>10,11</sup> It should be noted that such matrix stiffness effects have always been investigated for relatively “thick” gels (i.e., gels of at least 70  $\mu\text{m}$  in thickness). Whether this would remain valid for thin gels (ranging from nanometer to micrometer thicknesses) has barely been investigated because of the difficulty of preparing thin gels of controlled thickness and with different stiffnesses.<sup>5</sup>

In the biomaterial applications, polyelectrolyte multilayer (PEM) films are increasingly recognized as being a powerful tool to control key cellular processes.<sup>12–14</sup> These surface coatings can be deposited easily and have several different properties. For instance, a specific hormone, the  $\alpha$ -melanin-stimulating hormone ( $\alpha$ -MSH) can be grafted to a polyelectrolyte and be embedded in a film so as to induce the production of  $\alpha$ -melanocortin by melanoma cells.<sup>15</sup> Furthermore, the hydration and swellability

\* Corresponding author. E-mail: catherine.picart@univ-montp2.fr. Phone: (33)-(0)4-67-14-37-42. Fax: (33)-(0)4-67-14-42-86.

<sup>†</sup> Institut National de la Santé et de la Recherche Médicale, Université Louis Pasteur.

<sup>‡</sup> Albert-Ludwigs-Universität.

<sup>§</sup> UMR 7514 CNRS-ULP.

<sup>||</sup> Institut Charles Sadron, Université Louis Pasteur.

(1) Wong, J.; Leach, J.; Brown, X. *Surf. Sci.* **2004**, *570*, 119–133.

(2) Georges, P. C.; Janmey, P. A. *J. Appl. Physiol.* **2005**, *98*, 1547–1553.

(3) Pelham, R. J., Jr; Wang, Y. L. *Proc. Natl. Acad. Sci. U.S.A.* **1997**, *94*, 13661–13665.

(4) Engler, A. J.; Griffin, M. A.; Sen, S.; Bonnemann, C. G.; Sweeney, H. L.; Discher, D. E. *J. Cell Biol.* **2004**, *166*, 877–887.

(5) Thompson, M. T.; Berg, M. C.; Tobias, I. S.; Rubner, M. F.; Van Vliet, K. *J. Biomaterials* **2005**, *26*, 6836–6845.

(6) Richert, L.; Engler, A. J.; Discher, D. E.; Picart, C. *Biomacromolecules* **2004**, *5*, 1908–1916.

(7) Engler, A.; Bacakova, L.; Newman, C.; Hategan, A.; Griffin, M.; Discher, D. E. *Biophys. J.* **2004**, *86*, 617–628.

(8) Lo, C. M.; Wang, H. B.; Dembo, M.; Wang, Y. L. *Biophys. J.* **2000**, *79*, 144–152.

(9) Wong, J. Y.; Velasco, A.; Rajagopalan, P.; Pham, Q. *Langmuir* **2003**, *19*, 1908–1913.

(10) Genes, N. G.; Rowley, J. A.; Mooney, D. J.; Bonassar, L. J. *Arch. Biochem. Biophys.* **2004**, *422*, 161–167.

(11) Rowley, J. A.; Mooney, D. J. *J. Biomed. Mater. Res.* **2002**, *60*, 217–223.

(12) Groth, T.; Lendlein, A. *Angew. Chem., Int. Ed.* **2004**, *43*, 926–928.

(13) Jessel, N.; Schwinté, P.; Falvey, P.; Darcy, R.; Haikel, Y.; Schaaf, P.; Voegel, J.-C.; Ogier, J. *Adv. Funct. Mater.* **2004**, *14*, 174–182.

(14) Boura, C.; Muller, S.; Vautier, D.; Dumas, D.; Schaaf, P.; Claude Voegel, J.; Francois Stoltz, J.; Menu, P. *Biomaterials* **2005**, *26*, 4568–4575.

of the films influence cell adhesion,<sup>16</sup> as does the hydrophobicity/hydrophilicity,<sup>17</sup> which can be controlled by carefully choosing the polymers used in the buildup. The grafting of adhesive peptides such as RGD is another way to change the film adhesive properties.<sup>18,19</sup> Recently, several studies suggested that mechanical properties of the films have a great influence on cell adhesion, both for cell lines and for primary cells.<sup>5,20,21</sup> Strategies for increasing film stiffness include the incorporation of nanocolloids in the films<sup>21</sup> or building films at different pH for a given polycation/polyanion pair.<sup>5</sup> Another strategy makes use of a water-soluble cross-linking agent.<sup>20</sup> So far, native (or non-cross-linked films) were compared to cross-linked films at a fixed concentration of the cross-linking agent. Primary chondrocytes were shown to deform native films, whereas they can anchor durably on cross-linked films.<sup>22</sup> It would be interesting to prepare films of tunable elasticity that cover a large range of Young's moduli and to investigate whether the strong influence of mechanical properties on cell behavior found for 3D gels remains valid for 2D films that are much thinner (in the micrometer range). This effect, which is often called the substrate mechanical effect, has so far been mostly investigated for PDMS, polyacrylamide, and alginate gels<sup>1</sup> and has barely been investigated for other types of materials such as thin polymer films.<sup>5,6</sup> The PEM films in general, and (PLL/HA) films in particular, represent a new way to address this question.

The possibility of varying the surface mechanical properties by PEM film deposition would open new routes in the control of cellular processes over a wide range of biomaterial surfaces ranging from metals and ceramics to 3D polymeric matrices. Furthermore, because it is possible to prepare biocompatible PEM films, it would be possible to investigate the surface mechanical effects under in vivo conditions and to envision future applications of such films.

The present work is precisely aimed at varying the elasticity of PEM films made of PLL and hyaluronan (PLL/HA films) and at investigating the adhesion of cells deposited on these films. To this end, we used a cross-linking protocol based on carbodiimide chemistry (i.e., 1-ethyl-3-(3-(dimethylamino)-propyl)carbodiimide (EDC)) in combination with *N*-hydroxysulfosuccinimide (s-NHS) and cultured chondrosarcoma cells on films cross linked with EDC solutions of various concentrations.

To our knowledge, this is the first study aimed at elucidating the role of thin film mechanical properties (with film thickness in the micrometer range) in cell adhesion over a large range of film stiffness for films built in a given medium (at fixed pH) and subsequently cross linked to various degrees.

## Experimental Section

### Polyelectrolyte Solutions and Automated Buildup of the Films.

The preparation of solutions of poly(L-lysine) (PLL, 30 kDa, Sigma, France) and hyaluronan (HA, 400 kDa, Bioiberica, Spain) and the

buildup of (PLL/HA)<sub>*i*</sub> films (where *i* corresponds to the number of layer pairs) was described in a former article.<sup>23</sup> PLL and HA were dissolved at 1 mg/mL in a 0.15 M NaCl aqueous solution at pH 6–6.5. During film construction, all of the rinsing steps were performed with the 0.15 M NaCl aqueous solution at pH 6–6.5. The PEM films made either of 12- or 24-layer pairs were prepared with a dipping machine (Dipping Robot DR3, Kierstein GmbH, Germany) on 12 mm glass slides (VWR Scientific, France) as previously described.<sup>20</sup>

**Film Cross-Linking Procedure and Characterization by Fourier Transform Infrared Spectroscopy.** For the chemical cross linking of the films, a previously published protocol that was applied to (PLL/HA)<sub>*i*</sub> films<sup>20</sup> was again followed. It is based on the reaction of activated carboxylic sites with primary amine groups<sup>24</sup> in the presence of a water-soluble carbodiimide (EDC) and of s-NHS (both purchased from Sigma). Briefly, EDC was dissolved at pH 5 in a NaCl aqueous solution at various final concentrations (varying from 1 to 200 mg/mL). s-NHS was dissolved in the same solution at the final constant concentration of 11 mg/mL. The (PLL/HA)<sub>12</sub>- or (PLL/HA)<sub>24</sub>-coated glass slides were introduced in 24-well culture plates and put in contact with respectively 0.5 or 1 mL of the EDC/s-NHS mixture during 18 h at 4 °C. Rinsing was performed three times with a 0.15 M NaCl solution for 1 h at pH 8.

For film cross-linking characterization, (PLL/HA)<sub>8</sub> films deposited on a ZnSe crystal were investigated by in situ Fourier transform infrared (FTIR) spectroscopy in attenuated total reflection (ATR) mode with an Equinox 55 spectrophotometer (Bruker, Wissembourg, France). The experiments were performed in a deuterated 0.15 M NaCl solution at pH 6 for the film buildup and at pH 5 for the cross-linking reaction. The measuring cell was flushed with mixed EDC/s-NHS solutions (4 mL each). The parameters and configuration used for the acquisition during the cross-linking reaction have already been given in detail.<sup>20</sup> Spectra were acquired before, during, and after cross linking. (A single experiment was conducted for each EDC concentration, except for concentrations of 5, 35, and 100 mg/mL for which two experiments were performed to check the reproducibility of the cross linking.) The integral of the EDC band was calculated using OPUS 2 analysis software (Bruker, Wissembourg, France).

**Measurement of Young's Modulus by an AFM Using a Colloidal Probe.** The measurements aimed at the determination of the elasticity of the films were performed on (PLL/HA)<sub>24</sub> films using a homemade AFM working in indenter-type mode (IT-AFM). This number of layer pairs was chosen because these films can be easily visualized by confocal microscopy and their thickness can be measured<sup>6</sup> (for input in the curve-fitting procedure). The probe was constituted of a borosilicate sphere of 5 μm diameter fixed to the cantilever whose spring constant was either 0.06 or 0.38 N m<sup>-1</sup> as indicated by the manufacturer (BioForce, Nanosciences Inc., Ames, IA) and confirmed by the thermal fluctuation technique.<sup>25</sup>

The measurement procedure was essentially the same as that described by Richert et al.<sup>6</sup> All experiments were performed in a liquid environment (i.e., the films were immersed in a drop of 0.15 M NaCl aqueous solution). The piezodrives of the apparatus, onto which either a bare glass slide or a glass slide coated with a film was deposited, was previously calibrated interferometrically at a given frequency of the applied driving voltage.<sup>26</sup> To calibrate the photodiode, the probe was placed into contact with a bare glass slide. Because this latter is virtually infinitely hard, the probe follows the piezodrives movement. However, the expansion of the piezo-ceramic is frequency-dependent so that its calibration factor had to be corrected following the method described by Rutland et al.<sup>27</sup>

(15) Chluba, J.; Voegel, J. C.; Decher, G.; Erbacher, P.; Schaaf, P.; Ogier, J. *Biomacromolecules* **2001**, *2*, 800–805.

(16) Mendelsohn, J. D.; Yang, S. Y.; Hiller, J.; Hochbaum, A. I.; Rubner, M. F. *Biomacromolecules* **2003**, *4*, 96–106.

(17) Salloum, D. S.; Olenych, S. G.; Keller, T. C.; Schlenoff, J. B. *Biomacromolecules* **2005**, *6*, 161–167.

(18) Berg, M. C.; Yang, S. Y.; Hammond, P. T.; Rubner, M. F. *Langmuir* **2004**, *20*, 1362–1368.

(19) Picart, C.; Elkaim, R.; Richert, L.; Audoin, F.; Da Silva Cardoso, M.; Schaaf, P.; Voegel, J.-C.; Frisch, B. *Adv. Funct. Mater.* **2005**, *15*, 83–94.

(20) Richert, L.; Boulmedais, F.; Lavalle, P.; Mutterer, J.; Ferreux, E.; Decher, G.; Schaaf, P.; Voegel, J.-C.; Picart, C. *Biomacromolecules* **2004**, *5*, 284–294.

(21) Koktysh, D. S.; Liang, X.; Yun, B. G.; Pastoriza-Santos, I.; Matts, R. L.; Giersig, M.; Serra-Rodríguez, C.; Liz-Marzán, L. M.; Kotov, N. A. *Adv. Funct. Mater.* **2002**, *12*, 255–265.

(22) Richert, L.; Schneider, A.; Vautier, D.; Jessel, N.; Payan, E.; Schaaf, P.; Voegel, J.-C.; Picart, C. *Cell Biochem. Biophys.*, in press, 2005.

(23) Picart, C.; Lavalle, P.; Hubert, P.; Cuisinier, F. G.; Decher, G.; Schaaf, P.; Voegel, J.-C. *Langmuir* **2001**, *17*, 7414–7424.

(24) Hermanson, G. T. *Bioconjugate Techniques*; Academic Press: San Diego, CA, 1996; pp 169–176.

(25) Lévy, R.; Maaloum, M. *Nanotechnology* **2002**, *13*, 33–37.

(26) Hemmerle, J.; Altmann, S. M.; Maaloum, M.; Horber, J. K.; Heinrich, L.; Voegel, J. C.; Schaaf, P. *Proc. Natl. Acad. Sci. U.S.A.* **1999**, *96*, 6705–6710.

(27) Rutland, M. W. T.; Attard, J. W. G. *J. Adhes. Sci. Technol.* **2004**, *18*, 1199–1215.



Furthermore, to check for eventual viscosity effects, the indentation experiments on a given film were repeated at several different approach velocities (each at a different location on the film surface). The piezodriven position–cantilever deflection curves recorded at the various approach velocities were analyzed using the Hertz model for a spherical probe and eventually corrected for finite film thickness.<sup>6,28</sup> Difficulties arising in the fitting of the parts of the curves corresponding to the largest indentations led us to modify the Hertz expression by multiplying it by an empirical function that tends toward unity as the indentation tends toward zero. This had the advantage of an appreciably improved fit of the experimental curves with the consequence of a better positioning of the film–probe contact point and especially a better evaluation of the Young's modulus,  $E_0$ , in the low-indentation domain.<sup>29</sup> This parameter reflects the superficial elasticity of the film, which is assumed to be its relevant characteristic as far as cell adhesion is concerned.

Except for the native film and the weakly cross-linked films ( $C_{EDC} \leq 2 \text{ mg mL}^{-1}$ ), no tendency for  $E_0$  to grow with the approach velocity was visible. For the native film or weakly cross-linked films, the apparent modulus tended to a plateau as the approach velocity decreased, which reflects the gradual decline of the viscous contribution to the force exerted by the film on the penetrating probe. The estimates of  $E_0$  reported in Figure 5 are averages over the approach velocities (6 to 16 values for a given EDC concentration), where  $E_0$  is reasonably constant with respect to the approach velocity and the error bars represent the standard deviation of these samples.

**Wettability Measurements.** The wettability measurements were performed with a Digidrop ASE (GBX, Romans, France) that is a pendant-drop apparatus using a video digital image processing technique. The contact angle was determined at 25°C with Visilog image analysis software (Neosis, France).<sup>30</sup> The samples were first rinsed with water and dried under a nitrogen flow for 5 min. The contact angles of ultrapure water droplets deposited on the PEM film surfaces were measured. Each experiment was performed on three different film-coated slides for each film type.

**Atomic Force Microscopy (AFM) Imaging.** Atomic force microscopy images were obtained in contact mode in air with the Nanoscope IV from Veeco (Santa Barbara, CA).<sup>31</sup> Deflection and height mode images are scanned simultaneously at a fixed scan rate (2 Hz) with a resolution of 512 pixels  $\times$  512 pixels. The mean roughness of the films was calculated according to

$$R = \frac{1}{N_x N_y} \sum_{i=1}^{N_x} \sum_{j=1}^{N_y} |z_{ij} - z_{\text{mean}}|$$

where  $z_{ij}$  is the height of a given pixel,  $z_{\text{mean}}$  is the average height of the pixels, and  $N_x$  and  $N_y$  are the numbers of pixels in the  $x$  and  $y$  directions. The  $2 \mu\text{m} \times 2 \mu\text{m}$  images were subdivided into four areas for roughness calculation.

**Cell Culture and Viability (Trypan Blue Viability Test).** HCS-2/8 human chondrosarcoma cells were grown and subsequently deposited on the different films as described in a former article.<sup>20</sup> The (PLL/HA)<sub>12</sub>, either native or cross linked with EDC/s-NHS, was deposited on 14 mm glass slides that were put in a 24-well culture plate. The number of cells deposited in each well was  $3 \times 10^4$ . Three independent experiments were performed. Three wells per PEM film type were prepared in each experiment. The cells were observed by means of a Nikon Eclipse TE200 microscope with a 10 $\times$  objective. Three images per slide were taken with a DXM1200 camera and analyzed using Image J software (Rasband WS, NIH Bethesda). The mean cell area for about 70 cells was calculated for each EDC concentration.

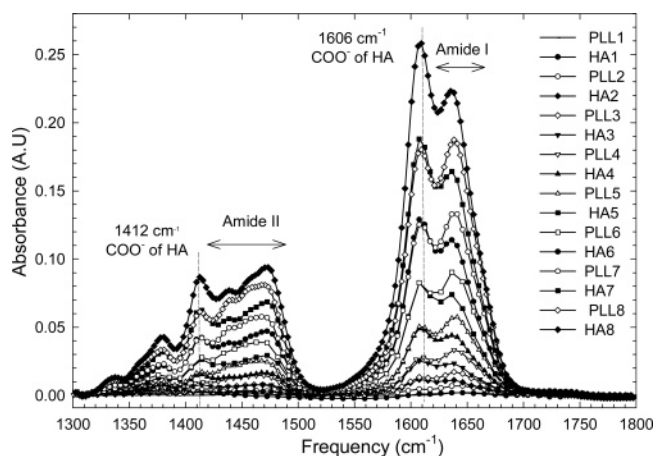


**Figure 1.** ATR-FTIR spectra of a (PLL/HA)<sub>8</sub> film during its buildup. The spectra are taken after each PLL or HA adsorption (after the rinsing step). The carboxylic peaks (1606 and 1412  $\text{cm}^{-1}$ , respectively) and the amide I and II bands (1600–1675 and 1400–1500  $\text{cm}^{-1}$ , respectively) can be clearly identified.

A trypan blue viability test was also performed. After 24 h or 5 days of culture on the different films, the medium was carefully removed, and the cells were washed with PBS before being detached with a trypsin/EDTA solution (Gibco BRL, U.K.). Then, trypan blue was added, and the noncolored cells (the living ones) were counted with a Neubauer cell. This viability test was performed twice (with three wells per film condition in each experiment). The statistical significance was determined by Kruskal–Wallis one-way analysis of variance. The tests were performed with SigmaStat 2.0 (Jandel Corporation, Germany), with a rejection level of  $p = 0.05$ , on samples of size  $n = 12$ .

## Results

### Characterization of Film Cross Linking by FTIR-ATR.

Film growth and its subsequent cross linking was followed by FTIR. During the (PLL/HA)<sub>8</sub> film buildup investigated in D<sub>2</sub>O at pH 6.5, a spectrum is acquired after each deposited layer (Figure 1). Two main regions can be distinguished: the most intense band at 1600–1700  $\text{cm}^{-1}$  contains both the amide I band (C=O stretching) from HA and PLL peptide bonds and the peak attributed to the  $\text{—COO}^-$  asymmetric stretch from HA (1606  $\text{cm}^{-1}$ ), and the band in the 1380–1500  $\text{cm}^{-1}$  region corresponds to the amide II vibrations (NH bending) of HA and PLL peptide bonds and to the  $\text{—COO}^-$  symmetric stretch (1412  $\text{cm}^{-1}$ ) of HA.<sup>32</sup>

To investigate the effect of various EDC concentrations on the (PLL/HA)<sub>8</sub> film spectrum, the EDC/sNHS solutions were put in contact with the films. The reaction was followed over a 10 h period, during which a spectrum was taken every 20 min. Figure 2 shows the time evolution of the spectrum for a (PLL/HA)<sub>8</sub> film after contact with the cross-linking solution at an EDC concentration of either 20 or 100  $\text{mg/mL}$ . These spectra evolve as soon as the film is brought into contact with the EDC/s-NHS solution. During the reaction, the carboxylic peaks at 1606 and 1412  $\text{cm}^{-1}$  and the band at 1675–1720  $\text{cm}^{-1}$  decreased, whereas at the same time the intensity of other bands increased in the amide I (1600–1675  $\text{cm}^{-1}$ ) and amide II (1400–1500  $\text{cm}^{-1}$ ) regions. The decrease in the carboxylic peaks of HA and the concomitant increase in the amide bands suggest that reticulation did effectively occur because of the reaction between HA carboxyl groups and PLL ammonium groups. The band at 1675–1720  $\text{cm}^{-1}$  could be attributed to EDC by comparison with infrared spectra measured on solutions of s-NHS, EDC, and mixtures of s-NHS with EDC in D<sub>2</sub>O (data not shown). Whereas

(28) Dimitriadis, E. K.; Horkay, F.; Maresca, J.; Kachar, B.; Chadwick, R. S. *Biophys. J.* **2002**, *82*, 2798–2810.

(29) Francius, G.; Hemmerle, J.; Ohayon, J.; Schaaf, P.; Voegel, J.-C.; Picart, C.; Senger, B. *Microsc. Res. Tech.*, in press, 2005.

(30) Schreyeck, G.; Marie, P. *Langmuir* **1999**, *15*, 8212–8219.

(31) Lavalle, P.; Gergely, C.; Cuisinier, F.; Decher, G.; Schaaf, P.; Voegel, J.-C.; Picart, C. *Macromolecules* **2002**, *35*, 4458–4465.

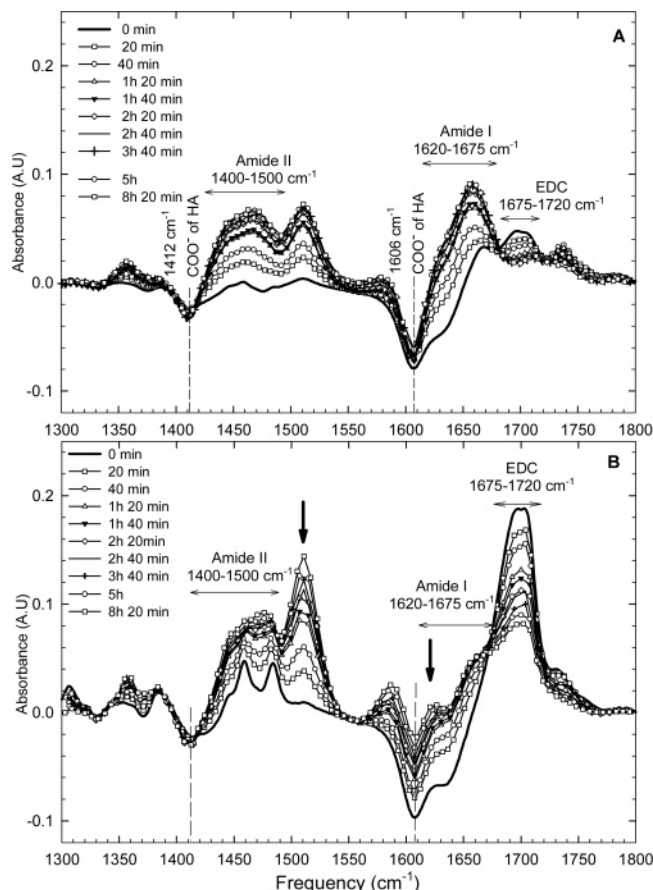


**Figure 2.** ATR-FTIR spectra acquired during the cross-linking reaction at EDC concentrations of (A) 20 and (B) 100 mg/mL. The evolution of the difference between the actual spectra during contact with the EDC/s-NHS solution and the spectrum recorded for (PLL/HA)<sub>8</sub> is represented as a function of the contact time. (The contribution of the PEM film was subtracted from the actual spectrum at each contact time.) The EDC band is located in the region of 1675–1720  $\text{cm}^{-1}$ .

the succinimide vibration of s-NHS ( $\text{O}=\text{C}-\text{N}-\text{C}=\text{O}$ ) shows up at 1715  $\text{cm}^{-1}$  on our spectrum,<sup>34,35</sup> EDC in solution shows an unexpected band at 1595–1705  $\text{cm}^{-1}$  that could be explained only by partial hydrolysis and consequent formation of an additional urea derivative (amide  $-\text{NH}-(\text{C}=\text{O})-\text{NH}-$ ), giving rise to a carbonyl vibration.<sup>36–38</sup> The doublet at 1460 and 1481  $\text{cm}^{-1}$  could be assigned to the two NH bending vibrations (amide II) of this amide. Interestingly, mixtures of EDC with NHS, at increasing concentration of EDC, show two new bands at about 1620 and 1510  $\text{cm}^{-1}$  (vertical arrows), which could be tentatively attributed respectively to amide I and amide II bands resulting from coupling between amino groups and carboxyl groups generated by the hydrolysis of both EDC and NHS.<sup>39–41</sup> These bands continue to grow along the experiment.

(32) Haxaire, K.; Marechal, Y.; Milas, M.; Rinaudo, M. *Biopolymers* **2003**, 72, 10–20.

(33) Haxaire, K.; Marechal, Y.; Milas, M.; Rinaudo, M. *Biopolymers* **2003**, 72, 149–161.

(34) Pistorius, A. M.; Groenen, P. J.; De Grip, W. J. *Int. J. Pept. Protein Res.* **1993**, 42, 570–577.

(35) Xiao, S.; Brunner, S.; Wieland, M. *J. Phys. Chem. B* **2004**, 108, 16508–16517.

(36) Bott, R.; Smith, G.; Wermuth, U.; Dwyer, N. *Aust. J. Chem.* **2000**, 53.

(37) Grabarek, Z.; Gergely, J. *Anal. Biochem.* **1990**, 185, 131–135.

(38) Timkovich, R. *Anal. Biochem.* **1977**, 79, 135–143.

(39) Konuklar, F. A.; Aviyente, V.; Ruiz Lopez, M. F. *J. Phys. Chem. A* **2002**, 106, 11205–11214.

(40) Aylin, F.; Konuklar, S.; Aviyente, V. *Org. Biomol. Chem.* **2003**, 1, 2290–2297.

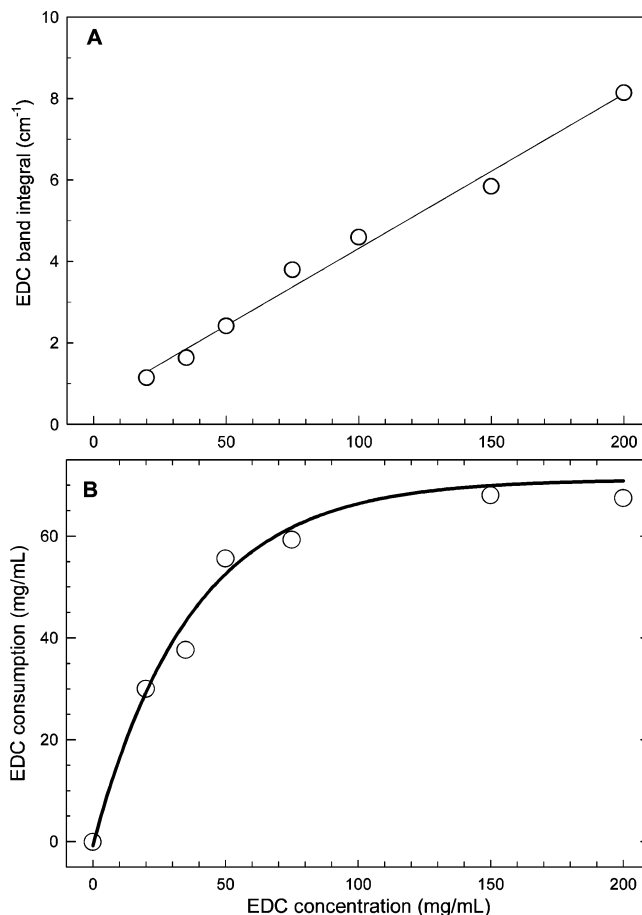


**Figure 3.** (A) Integral of the EDC band (1675–1720  $\text{cm}^{-1}$ ) obtained after the injection of the EDC/s-NHS solution in the measuring cell (time zero corresponding to the first acquisition), plotted as a function of the EDC concentration for (PLL/HA)<sub>8</sub> films. The integral is directly proportional to the EDC concentration. (B) EDC consumption (i.e., difference between the integral of the EDC band at the final acquisition and that at the first acquisition) as a function of the EDC concentration.

On the reticulation spectra, the decrease of the EDC/s-NHS mixed band (1675–1720  $\text{cm}^{-1}$ ) during the reaction is representative of EDC molecule consumption. We could verify that this band integral, at the beginning of the reaction (corresponding to the first acquisition), is directly proportional to the EDC initial concentration (Figure 3A). Then, the EDC consumption was estimated by considering, for each EDC concentration, the difference between the band integral at the end of the reaction and that at the beginning of the reaction. This integral was converted into a value for the EDC consumption by means of the linear regression obtained in Figure 3A. It comes out that the EDC consumption follows an exponential asymptotic law as a function of the initial EDC concentration (Figure 3B). The plateau is reached at about 70 mg/mL, which indicates that not all of the EDC molecules are consumed for the highest EDC concentrations.

The differences between the final spectra (after rinsing, the films that have been in contact for 10 h with the EDC/s-NHS solution) and the spectra of the native films before contact with the EDC/s-NHS solution are also represented for all of the EDC concentrations investigated (Figure 4). First, one can observe that the EDC/s-NHS band totally disappeared after the final rinsing step, which indicates that no free EDC and s-NHS molecules remain in the film. Second, one can notice that the amide I region (1600–1675  $\text{cm}^{-1}$ ) increase is not proportional to the EDC

(41) Shen, G.; Anand, M. F.; Levicky, R. *Nucleic Acids Res.* **2004**, 32, 5973–5980.

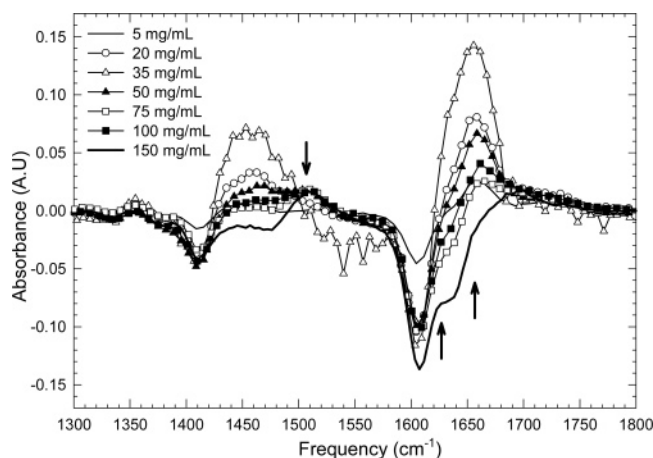


**Figure 4.** ATR-FTIR spectra of (PLL/HA)<sub>8</sub> films cross linked at various EDC concentrations. The difference between the two spectra (before and after cross linking) is represented for increasing EDC concentrations (5, 20, 35, 50, 75, 100, and 150 mg/mL).

concentration. At 5 mg/mL EDC, there is only a slight evolution in the spectrum upon cross linking. The maximum of the band increased for concentrations up to about 35 mg/mL and then decreased again. At high EDC concentration (100 mg/mL), the s-NHS/EDC band at 1675–1720 cm<sup>-1</sup> is initially very high, indicating a high proportion of hydrolysis. Two peaks are clearly visible in the amide I region (at 1650 and 1620 cm<sup>-1</sup>), and a second peak increases strongly in the amide II region at about 1510 cm<sup>-1</sup> beside the normal peptide amide II band at 1460 cm<sup>-1</sup> (vertical arrows). This could be explained by the formation of side products arising from the coupling of hydrolyzed s-NHS and EDC that could generate mixed reticulation patterns. Although much smaller, these side reactions are already present at 20 mg/mL EDC as can be seen in the spectra.

**Film Stiffness as a Function of EDC Concentration.** The surface mechanical properties of the (PLL/HA)<sub>24</sub> films were investigated by means of the AFM colloidal probe indentation technique. This technique is now commonly used to measure the local elastic moduli of soft and biological materials.<sup>28,42,43</sup> The value of the surface Young's modulus,  $E_0$ , is given as a function of the EDC concentration in Figure 5. As can be observed,  $E_0$  exhibits exponential growth toward a plateau value and levels off at a value on the order of 400 kPa for an EDC concentration of about 50 mg/mL. It is therefore possible to prepare films over a wide range of the Young's moduli by simply varying the cross-linker concentration.

**Chondrosarcoma Adhesion onto the Cross-Linked Films.** Chondrosarcoma cells were grown on the native (i.e., un-cross-linked) and cross-linked films (CL films) made of 12-layer pairs ( $\sim 1 \mu\text{m}^{23}$ ) ending with HA. Cell adhesion and growth was followed over a 5 day period. Images of the cells that have adhered on top of the films have been taken (Figure 6), and a trypan blue viability test was performed after 24 h and 5 days in culture (Figure 7).

One can observe by light microscopy that native films are unfavorable for cell adhesion as previously evidenced,<sup>20</sup> whereas the cross-linked ones are more favorable, though the positive effect of cross linking is strongly dependent on the EDC concentration (Figure 6). Whereas only a few cells remained on the films cross linked at low EDC concentration, the number of

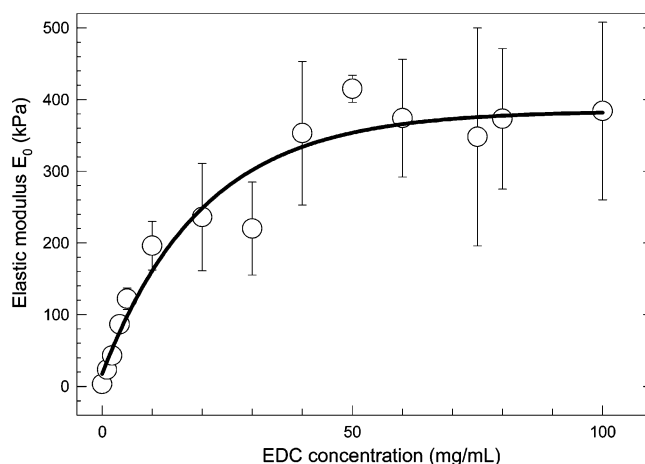


**Figure 5.** Surface Young's modulus  $E_0$  determined by the AFM nanoindentation technique for various EDC concentrations up to 100 mg/mL. An exponential asymptotic fit to the data is also represented (thick line). The error bars represent the standard deviation of 6–16 measurements of  $E_0$  corresponding to various approach velocities. (See Experimental Section for further details.)

cells increased as the EDC concentration increased as shown by the continuous increase in cell adhesion at 24 h as revealed by the trypan blue test (Figure 7A). The statistical analysis performed on these data showed that the number of living cells corresponding to concentrations up to 50 mg/mL was significantly different from the number of living cells at the highest EDC concentration (200 mg/mL). Not only did the initial cell number increase, but cell spreading also increased as a function of EDC concentration (Figures 6 and 8). The cell spreading area is generally assumed to give an indication of cell adhesion (but not cell viability). At the highest EDC concentrations (above 100 mg/mL), all of the cells are well spread. Clearly, cell spreading increases when the EDC concentration is increased, and the data can be well fitted by an exponential asymptotic law (Figure 8).

After 5 days, the number of living cells has increased for all EDC concentrations. Here again, the trend toward enhanced viability at elevated EDC concentrations is clearly visible (Figure 7B). The highest EDC concentration has a significant effect on the number of living cells as compared to the native film and that cross linked at 1 and 35 mg/mL. It is worth noting that, because of the initially high cell adhesion onto the films cross linked at EDC concentrations above 50 mg/mL, the absolute numbers of adherent cells onto these films did not increase much over the 5 day period. This is related to the fast proliferation of these cells, which then stop to proliferate once they have reached confluence.

Finally, to directly correlate the superficial Young's modulus,  $E_0$ , and the spreading area, the measured  $E_0$  and the estimated spread area were plotted for various EDC concentrations (using the fit deduced from the experimental data of cell spreading versus EDC concentration) (Figure 9). The mean cell surface area increases as  $E_0$  increases up to a certain level where it tends to a plateau corresponding to a virtually infinitely hard substrate (glass).

## Discussion

The effect of substrate mechanics on cell adhesion and differentiation has been the subject of a number of recent investigations, mainly on PAAM, PDMS, and alginate gels.<sup>7–9,44</sup> It is now recognized for many cell types and for a wide range

(42) Engler, A.; Richert, L.; Wong, J. Y.; Picart, C.; Discher, D. E. *Surf. Sci.* **2004**, 570, 142–154.

(43) Mahaffy, R. E.; Park, S.; Gerde, E.; Kas, J.; Shih, C. K. *Biophys. J.* **2004**, 86, 1777–1793.

(44) Deroanne, C. F.; Lapiere, C. M.; Nusgens, B. V. *Cardiovasc. Res.* **2001**, 49, 647–658.



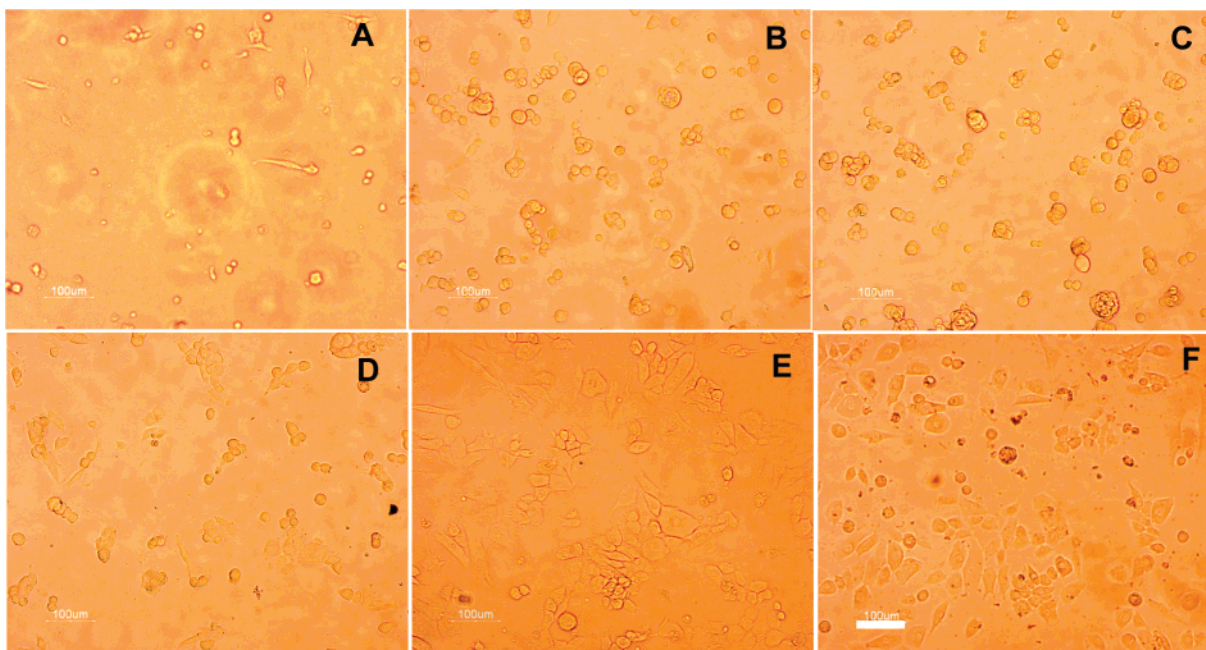


**Figure 6.** Microscopic observation of chondrosarcoma cells (at day 3) cultured on (PLL/HA)<sub>12</sub> films cross linked at various EDC concentrations: (A) 1, (B) 5, (C) 20, (D) 35, (E) 100, and (F) 200 mg/mL. Scale bar: 100  $\mu$ m.

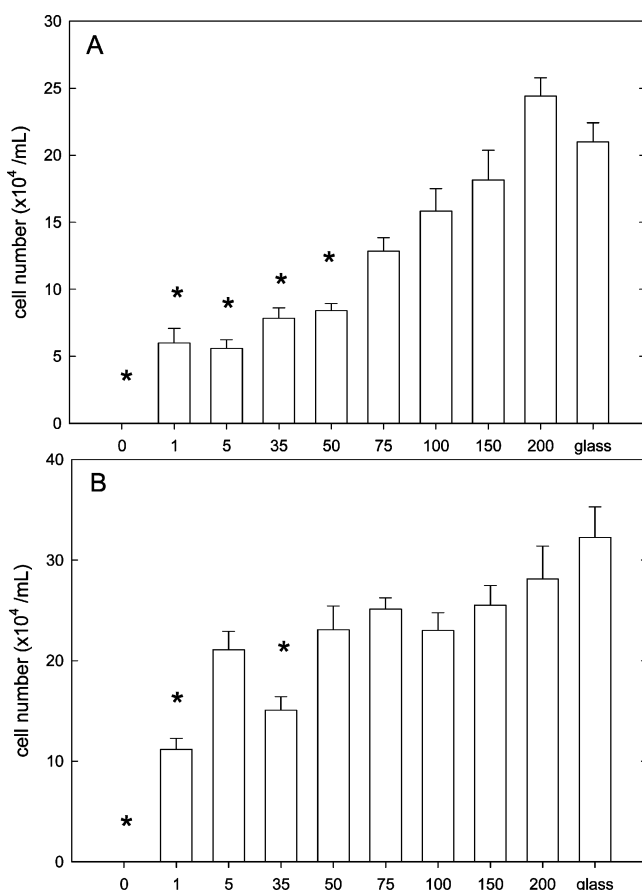


**Figure 7.** Results of the trypan blue test (cell viability) for chondrosarcoma cells cultured on (PLL/HA)<sub>12</sub> films cross linked at various EDC concentrations: (A) after 24 h and (B) after 5 days. Values and standard errors are obtained for three slides per film type. The adhesion was statistically different as compared to that at the concentration of 200 mg/mL in EDC (Kruskal–Wallis one-way analysis of variance,  $*p < 0.05$ ).

of film stiffnesses that the mechanical properties of a substrate, beside its chemistry and topography, are a key point in its adhesion

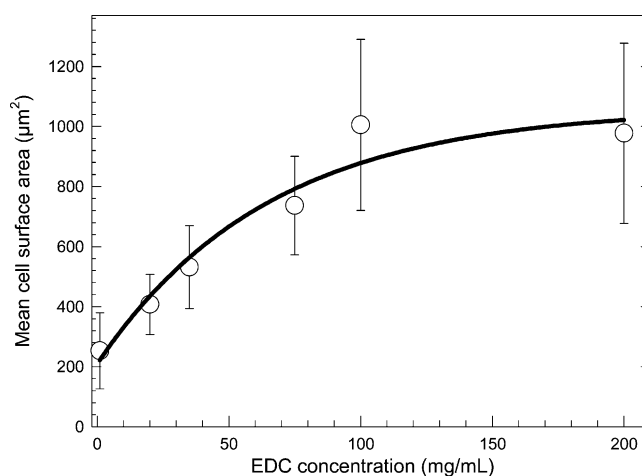


**Figure 8.** Spreading cell area measured for cells grown on (PLL/HA)<sub>12</sub> films cross linked at various EDC concentrations (at least 70 cells were analyzed for each condition) after 3 days in culture. Error bars are standard deviations.

properties.<sup>1</sup> For instance, the matrix stiffness has become increasingly recognized as playing a role in many cellular processes ranging from motility<sup>3,8</sup> to phagocytosis<sup>45</sup> and differentiation.<sup>44</sup> Not only do cells display a spreading preference for stiffer substrates but the cells prefer to migrate toward stiffer regions of a substrate, a phenomenon referred to as durotaxis.<sup>8</sup>

The effect of substrate mechanics on adhesion was checked for different cell types, such as fibroblasts, neurons,<sup>46</sup> and more recently smooth muscle cells.<sup>7,9</sup> These observations could be analyzed on the basis of gel softness: an extremely soft gel could be perceived by a cell as nearly fluid and therefore inadequate for sustaining an anchorage-dependent response.<sup>7</sup> Recently, the effect of substrate mechanics was also evidenced for chondrocytes grown on alginate gels over a modulus range of 10 to 130 kPa.<sup>10</sup> However, mechanical factors impact different

(45) Benigno, K. A.; Lo, C. M.; Wang, Y. L. *Methods Cell Biol.* **2002**, 69, 325–339.

(46) Flanagan, L. A.; Ju, Y. E.; Marg, B.; Osterfield, M.; Janmey, P. A. *Neuroreport* **2002**, 13, 2411–2415.

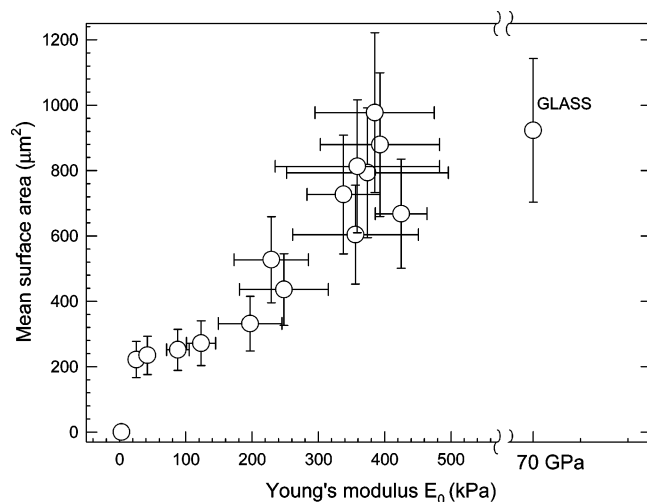


**Figure 9.** Correlation between the surface Young's modulus,  $E_0$ , and the spreading cell area. Error bars are standard deviations.

cell types in fundamentally different ways as recently demonstrated for fibroblasts, endothelial cells, and neutrophils.<sup>47</sup> In vivo, matrix stiffness may also play a role in various pathologies such as muscular dystrophies.<sup>4</sup> Theoretical work by Bischofs and Schwarz also underlines the crucial role of substrate stiffness in cell orientation in gels.<sup>48</sup>

Whether this substrate mechanical effect remains valid for different types of materials is an important question. In particular, PAAM gels, which are a nice model in vitro, cannot be implanted in vivo because of the known toxicity of the acrylamide monomer. The PEM films are a new type of coating whose thickness can be varied in the nanometer to micrometer range depending on the polyelectrolytes and buildup conditions used. In previous works, we have already provided evidence that the film mechanical properties can have an effect on cell adhesion.<sup>6,19,22</sup> In these works, films cross linked at a fixed EDC concentration (37.5 mg/mL) were compared to native films. The adhesion of chondrosarcoma cells, primary chondrocytes, osteoblasts, and neurons was drastically increased on the cross-linked films (at fixed EDC concentration) as compared to that on the native ones. Chondrocytes were able to exert forces and "pull" on the native films so as to make an imprint on the films.<sup>22</sup> In the present work, we extend the previous findings over a large range of film stiffnesses by varying the EDC concentration and by evaluating the corresponding Young's moduli of the films. In contrast to gels, there are only a few experimental techniques to study the mechanical properties of thin films, and AFM nanoindentation is the most widely used.<sup>49</sup> Rheometry and uniaxial stretching cannot be applied on nanometer- or micrometer-thick films.

In the present case, it was thus possible to show that cell adhesion depends on film stiffness (as measured by its surface Young's modulus) over the range available for (PLL/HA) films (3 to 400 kPa). Cell adhesion and the spreading area depended on film stiffness over the range investigated with the maximum of cell spreading reached at  $E_0 \approx 400$  kPa. The film stiffness of PEM films made of PLL/HA is in the range of 3–400 kPa, which is higher than that of pure PAAM (2–40 kPa) and of alginate gels (2–130 kPa) but below that of PDMS substrates

(12.5 kPa–2.5 MPa).<sup>1</sup> It has to be noted that this value for optimal spreading is 2 orders of magnitude higher than the minimum value for which cells spread nicely on PAAM gels (3 kPa).<sup>2</sup> Another important great difference is that fibroblasts were able to form confluent monolayers indistinguishable from those formed by cells on stiffer PAAM surfaces, whereas this was never observed for chondrosarcoma cells on cross-linked PEM films. The poor adherence on the softer films remains valid over the 5 day period of culture. The high softness/deformability of the native films may be related to the poor resistance of the films as cells are trying to pull on them and to the observation of a deformation zone.<sup>22</sup>

Other biopolymeric films were found to be highly nonadhesive for cells such as PLL/alginate,<sup>50</sup> chitosan/hyaluronan (poor adhesion of chondrocytes),<sup>51</sup> and poly(acrylic acid)/poly(allylamine hydrochloride)<sup>18,52</sup> (poor adhesion of fibroblasts). Recently, Thompson et al. used a similar AFM spectroscopic approach to measure the elastic modulus of (PAA/PAH) films built at different pH.<sup>5</sup> They found a much higher modulus ( $\sim 150$  MPa) for PAH/PAA films built at pH 6.5 than for films built at pH 2.5 ( $\sim 200$  kPa). Human microvascular endothelial cell density correlated with the Young's modulus ( $E$ ), and this density increased as  $E$  increased. These results confirm on a different system and for different buildup conditions the important role of the PEM film mechanical properties in cell adhesion. However, these authors also found a different cell adhesion response depending on the film ending layer with a systematically higher adhesion on PAA-terminated films than on PAH-terminated ones for all pH values investigated. In the present case, results were similar regardless of whether HA or PLL was the ending layer.<sup>20</sup> This may be ascribed to a higher softness of the PLL/HA films and to the exponential buildup mechanism of these films resulting from PLL diffusion and complex formation with an absence of layering,<sup>53</sup> in contrast to linearly growing films. By taking different polyelectrolyte pairs, it is thus possible to tune the film mechanical properties and to obtain an elastic modulus over 6 orders of magnitude, from a few kPa for the soft polysaccharide PEM films to several hundred MPa or even GPa for the stiff poly(styrene sulfonate)/poly(allylamine hydrochloride) films.<sup>54</sup>

Beside the mechanical properties of the films, other factors such as surface chemistry,<sup>55</sup> topography,<sup>56</sup> hydrophobicity,<sup>57</sup> and protein adsorption are likely to play a role in the cell response on cross-linked PEM films. The surface chemistry could also be slightly affected by the cross linking because this may play a role in the number of free chain ends within the architecture. The topography of the film may also be different. The interplay between all of these parameters may affect cell adhesion because changes in cell spreading are observed over the EDC concentration range of 50–200 mg/mL (Figure 8) whereas the Young's modulus is approximately constant in the same range (Figure 5). To check this point, the films cross linked at various EDC concentrations were imaged by AFM, and the film roughness was measured (Figure 10). Film roughness increases with EDC concentration

(50) Elbert, D. L.; Herbert, C. B.; Hubbell, J. A. *Langmuir* **1999**, *15*, 5355–5362.

(51) Richert, L.; Lavalle, P.; Payan, E.; Stoltz, J.-F.; Shu, X. Z.; Prestwich, G. D.; Schaaf, P.; Voegel, J.-C.; Picart, C. *Langmuir* **2004**, *1*, 284–294.

(52) Yang, S. Y.; Mendelsohn, J. D.; Rubner, M. F. *Biomacromolecules* **2003**, *4*, 987–994.

(53) Picart, C.; Mutterer, J.; Richert, L.; Luo, Y.; Prestwich, G. D.; Schaaf, P.; Voegel, J.-C.; Lavalle, P. *Proc. Natl. Acad. Sci. U.S.A.* **2002**, *99*, 12531–12535.

(54) Dubreuil, F.; Elsner, N.; Fery, A. *Eur. Phys. J. E* **2003**, *12*, 215–221.

(55) Castner, D. G.; Ratner, B. D. *Surf. Sci.* **2002**, *500*, 28–60.

(56) Dalby, M. J.; Yarwood, S. J.; Riehle, M. O.; Johnstone, H. J. H.; Affrossman, S.; Curtis, A. S. G. *Exp. Cell Res.* **2002**, *276*, 1–9.

(57) Vogler, E. A.; Bussian, R. W. *J. Biomed. Mater. Res.* **1987**, *21*, 1197–1211.

(47) Yeung, T.; Georges, P. C.; Flanagan, L. A.; Marg, B.; Ortiz, M.; Funaki, M.; Zahir, N.; Ming, W.; Weaver, V.; Janney, P. A. *Cell Motil. Cytoskeleton* **2005**, *60*, 24–34.

(48) Bischofs, I. B.; Schwarz, U. S. *Proc. Natl. Acad. Sci. U.S.A.* **2003**, *100*, 9274–9279.

(49) Bhushan, B. *Wear* **2001**, *250*, 1105–1123.



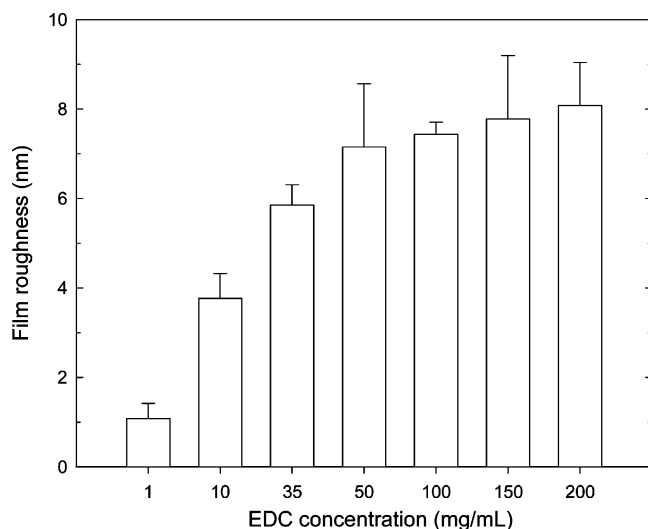


**Figure 10.** Film roughness (nm) as measured by AFM as a function of EDC concentration. Error bars are standard deviations (for eight different locations).

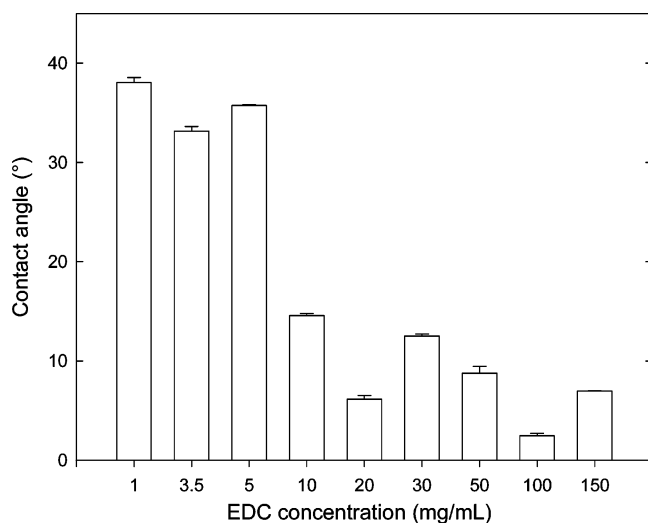


**Figure 11.** Water contact angle for films cross linked at increasing EDC concentrations.

from 1 nm toward a plateau value at about 7 nm for the 100 mg/mL concentration. Thus, conditions for good adhesion and proliferation correspond to the highest surface roughness. The specific effect of nanometer-scale roughness was recently shown to enhance cell adhesion.<sup>58</sup> For the (PLL/HA) cross-linked films, because the change in roughness is relatively moderate (from 1 to 7 nm) and the film is not structured topographically, the changes due to film roughness probably contribute only slightly to the important changes observed in adhesion.

Regarding the possible role of the hydrophobicity/hydrophilicity of the films, all of the films cross linked at EDC concentrations above 10 mg/mL have water contact angles below 12° and are hydrophilic (Figure 11). This parameter may affect cell spreading only slightly because it is precisely above this concentration that the highest changes in cell adhesion, mean spreading area, and the Young's modulus are observed. The present results are in contradiction with those presented by Saaloum et al.<sup>17</sup> in a recent study, where hydrophobic films were preferred for smooth muscle cell adhesion. Finally, protein adsorption and conformation may vary depending on the cross-linking rate, in particular, that due

to roughness, charge modifications, and changes in hydrophilicity. This particular point was recently investigated by several groups, which have quantified the density of adhesive molecules on substrata with different stiffness and found that ligand density does not vary significantly with cross-linking density.<sup>7,9</sup> In addition, Engler et al.<sup>7</sup> independently varied both substrate stiffness and ligand density and demonstrated that increases in adhesion ligand density do not compensate for low adhesion on soft gels. Regarding PEM films in particular, the adhesive or antiadhesive properties of PAA/PAH films were found to be independent of protein adsorption.<sup>16</sup>

All together, our results demonstrate the important role of film mechanics in cell adhesive properties. These results are important in the design of new biomaterial coatings for vascular surgery or other applications and could open new routes in the control of cellular behavior on biomaterial surfaces. Recently, we provided evidence that cross-linked chitosan/hyaluronan (CHI/HA) films are biocompatible and biodegradable in vivo for a longer time period than native ones.<sup>59,60</sup> The possibility of controlling the cross-linking density of the PEM films may be ideally combined with drug delivery. To this end, we are now working on the functionalization of these cross-linked films and have obtained encouraging preliminary results with an anti-inflammatory drug and with an antiproliferative drug (A. Schneider, in preparation). One could therefore envision preparing drug-eluting PEM films that contain a drug and also may interact with adherent cells in a beneficial way. Therefore, we possess PEM coatings with which it is possible to tune in a combined way the mechanical stiffness, biodegradability, cell adhesion, and bioactivity properties of PEM coatings.

## Conclusions

We have shown that it is possible to modulate the mechanical properties of hydrated PEM films. Film stiffness could be varied over 2 orders of magnitude by adjusting the cross-linker (EDC) concentration. Such a water-based protocol can be applied to a wide variety of films provided that they contain carboxylic and amine groups. The cross-linking reaction can be characterized by FTIR, and film stiffness can be measured by AFM nanoindentation, with the cross-linked films behaving as elastic media. The film mechanical properties have a strong influence on cell behavior, with stiff films being preferred in terms of cell adhesion and spreading. Such films are of interest for further studies including cell differentiation, cytoskeletal organization, and motility. It is also envisioned to study the mechanical properties of other polyelectrolyte pairs, particularly those made of polysaccharides only, and to combine mechanical and biodegradability properties.

**Acknowledgment.** This work has been partly supported by the Action Concertée Incitative "Nanosciences" (ACI NR204) from the Ministère de la Jeunesse, de l'Éducation Nationale et de la Recherche. G.F. is indebted to the Faculté de Chirurgie Dentaire of Strasbourg for financial support. We are grateful to Cosette Betscha for her technical assistance in the cell culture experiments and to Dr. Youri Arntz for his assistance in AFM imaging. We are grateful to Pascal Marie (Institut Charles Sadron, CNRS, Strasbourg) for access to the pendant drop apparatus. We thank Professor Dennis Discher (University of Pennsylvania) for fruitful discussions.

LA0521802

(58) Price, R. L.; Ellison, K.; Haberstroh, K. M.; Webster, T. J. *J. Biomed. Mater. Res.* **2004**, *70*, 129–138.

(59) Etienne, O.; Schneider, A.; Taddei, C.; Richert, L.; Schaaf, P.; Voegel, J.-C.; Egles, C.; Picart, C. *Biomacromolecules* **2005**, *6*, 726–733.

(60) Picart, C.; Schneider, A.; Etienne, O.; Mutterer, J.; Egles, C.; Jessel, N.; Voegel, J.-C. *Adv. Funct. Mater.* **2005**, November, 1771–1780.